research papers

Very first tests on SOLEIL regarding the Zn environment in pathological calcifications made of apatite determined by X-ray absorption spectroscopy

Dominique Bazin,[a]* Xavier Carpentier,[a,b] Olivier Traxer,[b] Dominique Thiaudière,[c] Andrea Somogyi,[c] Solenn Reguer,[c] Glenn Waychunas,[d] Paul Jungers[e] and Michel Daudon[e]

[a]Laboratoire de Physique des Solides, Bâtiment 510, Université Paris Sud, 91405 Orsay, France, [b]AP-HP, Hôpital Tenon, Service d'Urologie, 4 Rue de la Chine, 75020 Paris, France, [c]Synchrotron SOLEIL, L'Orme des Merisiers, Saint-Aubin, BP 48, 91192 Gif-sur-Yvette Cedex, France, [d]Lawrence Berkeley National Laboratory, MS 70R108B, 1 Cyclotron Road, Berkeley, CA 94720, USA, and [e]AP-HP, Hôpital Necker, Service de Biochimie A, 149 Rue de Sèvres, 75743 Paris Cedex 15, France. E-mail: bazin@lps.u-psud.fr

This very first report of an X-ray absorption spectroscopy experiment at Synchrotron SOLEIL is part of a long-term study dedicated to pathological calcifications. Such biological entities composed of various inorganic and/or organic compounds also contain trace elements. In the case of urinary calculi, different papers already published have pointed out that these oligo-elements may promote or inhibit crystal nucleation as well as growth of mineral. Use of this analytical tool specific to synchrotron radiation, allowing the determination of the local environment of oligo-elements and thus their occupation site, contributes to the understanding of the role of trace elements in pathological calcifications.

Keywords: X-ray absorption near-edge structure; pathological calcification; oligo-elements; kidney stones.

1. Introduction

Pathological calcifications, associated with very different pathologies ranging from atherosclerosis to gastric cancer (see, for example, Lairda *et al.*, 2006; Balestreri *et al.*, 1997), may be composed of various inorganic and/or organic compounds. If we restrict the scope of such biological entities to kidney stones, the principal components found for the mineral part, which have a hierarchical structure (Fratzl, 2002; Dujardin & Mann, 2002), are calcium oxalate (70% of the cases), calcium and magnesium phosphates (15%), uric acid (10%) and cystine (1%). By using analytical tools implemented at the hospitals and consistent with this chemical complexity, such as optical microscopy and infrared spectrophotometry, it is possible to relate their chemical nature and macrostructure to a distinct pathology. For example, in the case of urinary calculi, a link has been established between cystine and cystinuria, while struvite (magnesium ammonium phosphate) kidney stones, often called an 'infection stone', are usually caused by urinary tract infections with certain types of bacteria. It is also of note that such correlations can be far more subtle, *e.g.* the same chemical phases may be related to very different pathologies. In that case, an explanation can be found by taking into account the hierarchical structure of the mineral part.

An additional level of complexity is given by the presence of trace elements. Among them, some elements may play a role in crystal formation and/or organization of the stones owing to their special affinity for some crystalline species (Touryan *et al.*, 2004). In previous studies (Bazin & Rehr, 2003; Bazin *et al.*, 2006, 2007), we tried to classify these different elements through synchrotron radiation micro-X-ray fluorescence. Obviously the presence of major elements which form crystalline phases, *i.e.* Ca and S (S for cystine), are measured, then oligo-elements such as Sr and Se, but also 'metals of life' such as Fe, Cu and Zn, and finally pathological elements such as Pb. The presence of Sr is linked to the fact that Ca and Sr share the same column in the periodic table (similarly for S and Se). More precisely, the complete set of data which includes the different family of kidney stones (whewellite, weddelite, apatite, cystine, uric acid, struvite) is highly suggestive of a substitution process between calcium and the other metals (and not a catalytic one).

Table 1
Composition as given by Fourier-transform infrared spectroscopy (FTIR) and the origin of the ectopic calcification.

CA = carbonated calcium hydroxylapatite, MAP = magnesium ammonium phosphate (struvite), Prot = Protein, C1 = whewellite, C2 = weddellite, ACCP = amorphous carbonated calcium phosphate.

Sample	Origin of the calcification	Composition as given by FTIR
N 9009	Kidney	55% CA, 38% MAP, 3% Prot, 2% C2, 2% C1
N 13066	Kidney	79% CA, 15% ACCP, 4% Prot, 2% C1
N 13086	Prostatic	84% CA, 12% Prot, 4% C1
N 20208	Kidney	79% CA, 10% C2, 7% Prot, 4% C1

We focus the first report of X-ray absorption spectroscopy (XAS) experiments performed at SOLEIL on one of these oligo-elements, *i.e.* on Zn, in order to obtain more information on the substitution process. Different studies have already shown that XAS can be employed in order to determine the environment of one selected element through its absorption-edge features (Eichert *et al.*, 2005, 2007; Liou *et al.*, 2004; Siritapetawee & Pattanasiriwisawa, 2008). More precisely, information regarding the average coordination geometry as well as the average effective charge are available even for low Zn concentration materials (Bazin & Rehr, 2003).

2. Experimental

2.1. Material

The biological samples (Table 1) used in the present study came from French patients and were first characterized by infrared spectrophotometry using a Vector 22 (Bruker Spectrospin, Wissembourg, France) Fourier-transform infrared spectrometer according to the analytical procedure previously described (Daudon *et al.*, 1993; Estepa & Daudon, 1997).

2.2. XANES measurements

The stones were investigated either on the H10 (Gailhanou *et al.*, 2001) beamline at LURE (Orsay, France) or on the DIFFABS (Baudelet *et al.*, 2005) beamline at Synchrotron SOLEIL (St Aubin, France) in order to determine the electronic state as well as the coordination of Zn atoms. DIFFABS offers the possibility of studying the short- and medium-range structural characteristics of materials by the almost simultaneous combination of XAS and wide-angle X-ray scattering. DIFFABS, situated at the D13-1 bending magnet, is equipped with a focused monochromatic beam ('normal mode', energy range: 3–23 keV) provided by two bent Rh-coated mirrors and a double-crystal Si(111) sagitally focusing monochromator situated in the optic hutch. More details are available on the Synchrotron SOLEIL website. In our case the experiment was performed without using a focusing device (available at the end of 2008). X-ray absorption near-edge structure (XANES) spectra were normalized to an edge jump of unity. A prior removal of the background absorption was carried out by subtraction of a linear function extrapolated from the pre-edge region.

Following a monoelectronic description of the absorption phenomenon, electronic transitions are allowed between $1s$ and $4p$ levels but prohibited towards $3d$ levels (the dipole selection rule gives $\Delta l = +1$). In fact, hybridizations between $4p$ and $3d$ atomic orbitals allow transition between molecular orbitals with $3d$ and $4p$ mixed character. At this point we recall that for an octahedral symmetry the first unoccupied orbital, t_{1u}^*, possesses a $4p$ character and is associated with the main absorption jump for Zn K-edge spectra. The case for tetrahedral symmetry is more complicated (Rose *et al.*, 2001).

Some authors (Waychunas *et al.*, 2003; Giorgetti *et al.*, 1999; Wilkinson, 1987) have discussed extensively the form and the position of the Zn edge in compounds having different coordination sites. These features are sensitive to interatomic distances (Bianconi *et al.*, 1985) and/or coordination geometry (Jacquamet *et al.*, 1998). Also, the almost constant value of the edge position indicates a relatively constant value for the effective charge of the inserted zinc ions for all compounds.

In the case of an octahedral first-neighbour anion shell, a strong initial peak followed by a well defined second peak is measured (Fig. 1). Depending on the details of the overall structure, a small number of other contributions are also visible in the second peak. By comparison, tetrahedral Zn (in willemite and zincite) is associated with a more complex XANES structure. At least three well defined edge features can be visible.
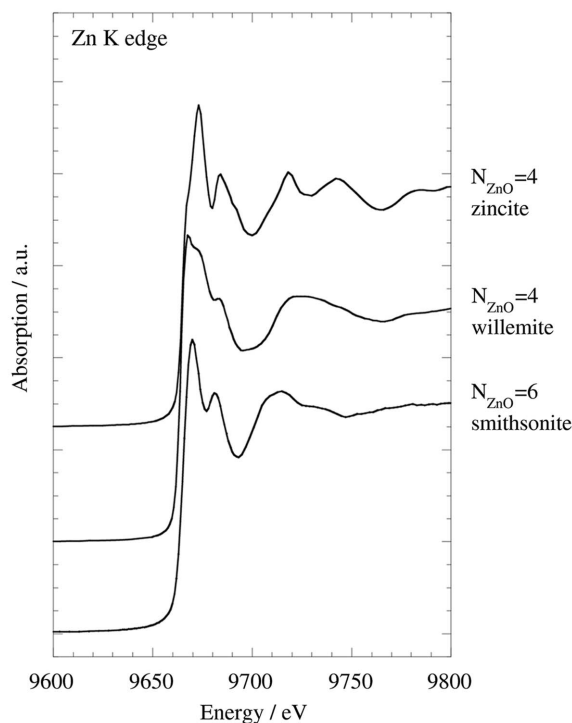
Figure 1
XANES spectra recorded at the Zn K-edge (9659 eV) for a set of references (zincite, zillemite, smithsonite). The zinc environment is indicated.
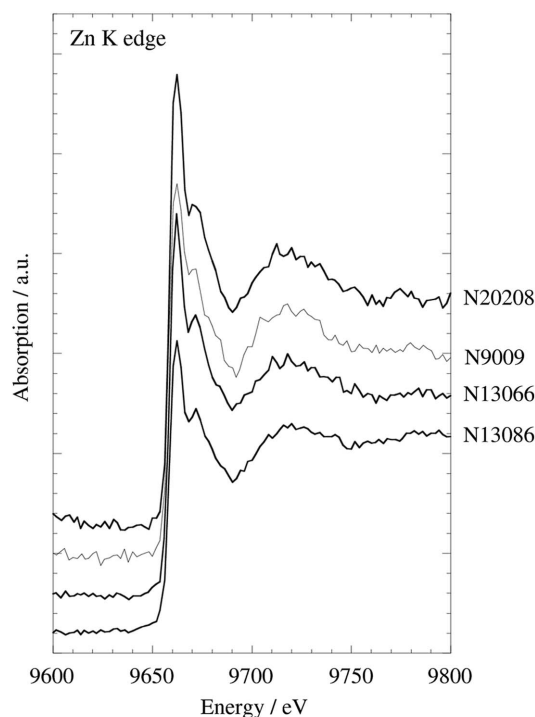
Figure 2
XANES spectra recorded at the Zn K-edge (9659 eV) for selected pathological samples.

3. Experimental data and discussion

In the case of our biological samples, powder neutron diffraction experiments have been performed (Daudon *et al.*, 2008). Although the background level is high owing to the hydrogen content of this biological sample, the high quality of the data allows a complete Rietveld-type refinement using a calcium hydroxylapatite, $Ca_{10}(PO_4)_6(OH)_2$, structural model with hexagonal space group $P6_3/m$ (Kay *et al.*, 1964; Elliott, 1994; Arcos *et al.*, 2004). In this structure, four Ca ions, at Ca(I) sites, lie along columns parallel to the *c* axis while six Ca atoms, positioned at Ca(II) sites, reside on the mirror planes. Thus, there are two distinct calcium environments (Okasinski *et al.*, 1999; Sowrey *et al.*, 2004): Ca(I), which is best described for the different calcium oxygen bonds as $N_{CaO} = 6$ ($R_{CaO} = 2.43$ Å) + $N_{CaO} = 3$ ($R_{CaO} = 2.79$ Å) coordination environment, and Ca(II), best described as either $N_{CaO} = 4$ ($R_{CaO} = 2.36$ Å) + $N_{CaO} = 2$ ($R_{CaO} = 2.51$ Å) + $N_{CaO} = 1$ ($R_{CaO} = 2.71$ Å) or $N_{CaO} = 5$ ($R_{CaO} = 2.35$ Å) + $N_{CaO} = 2$ ($R_{CaO} = 2.51$ Å) + $N_{CaO} = 1$ ($R_{CaO} = 2.71$ Å). Ca(I) and Ca(II) are present in a 2/3 ratio. Note also that, in the case of urinary calculi, calcium hydroxylapatite may contain a large amount of carbonate groups and thus is denominated as carbonate apatite.

Here, for all the four selected samples considered (Fig. 2), a constant value of the edge position is measured indicating a constant value for the effective charge of the zinc ions. Moreover, a careful examination of the XANES part of the absorption spectra indicates an octahedral complex much like that found in smithsonite. Thus, XAS indicates that Zn atoms are probably positioned mainly at the Ca(I) site.

At this point, additional development of the synchrotron radiation source as well as of the beamline are required in order to collect the EXAFS part of the X-ray absorption spectra and thus to better describe the site occupation of Zn. It is quite clear that only a combined analysis of the XANES and the EXAFS modulations will give a fine description of the zinc environment.

4. Conclusion

This very first set of experimental tests contributes to our understanding of the role of trace elements in concretions. By using analytical tools that are consistent with the chemical complexity of the sample, *i.e.* powder neutron diffraction for characterization of the matrix of biological apatite, and XAS for the determination of the coordination number and the electronic state of the oligo-elements (here Zn), information regarding the role of trace elements in the formation of the ectopic calcification will be given to the medical community. Finally, motivated by these initial observations, a second set of EXAFS experiments has been scheduled.

References

Arcos, D., Rodríguez-Carvajal, J. & Vallet-Regí, M. (2004). *Solid State Sci.* **6**, 987–994.
Balestreri, L., Canzonieri, V. & Morassut, S. (1997). *Clin. Imag.* **21**, 122–125.
Baudelet, F. *et al.* (2005). *Oil Gas Sci. Technol. Rev. IFP*, **60**, 849–874.
Bazin, D., Chevallier, P., Matzen, G., Jungers, P. & Daudon, M. (2007). *Urol. Res.* **35**, 179–184.
Bazin, D., Daudon, M., Chevallier, P., Rouzière, S., Elkaim, E., Thiaudière, D., Fayard, B., Foy, E., Albouy, P. A., André, G., Matzen, G. & Veron, E. (2006). *Ann. Biol. Clin.* **64**, 125–139.
Bazin, D. & Rehr, J. (2003). *Catal. Lett.* **87**, 85–90.
Bianconi, A., Fritsch, E., Calas, G. & Petiau, J. (1985). *Phys. Rev. B*, **32**, 4292–4295.
Daudon, M., Bader, C. A. & Jungers, P. (1993). *Scan. Microsc.* **7**, 1081–1095.
Daudon, M., Bazin, D., Jungers, P., André, G., Cousson, A., Chevallier, P., Véron, E. & Matzen, G. (2008). *J. Appl. Cryst.* Submitted.
Dujardin, E. & Mann, S. (2002). *Adv. Mater.* **14**, 775–788.
Eichert, D., Gregoratti, L., Kaulich, B., Marcello, A., Melpignano, P., Quaroni, L. & Kiskinova, M. (2007). *Anal. Bioanal. Chem.* **389**, 1121–1132.
Eichert, D., Salome, M., Banu, M., Susini, J. & Rey, C. (2005). *Spectrochim. Acta B*, **60**, 850–858.
Elliott, J. C. (1994). *Structure and Chemistry of the Apatites and Other Calcium Orthophosphates.* Amsterdam: Elsevier.
Estepa, L. & Daudon, M. (1997). *Biospectroscopy*, **3**, 347–355.
Fratzl, P. (2002). *Fib. Diff. Rev.* **210**, 31–319.
Gailhanou, M. *et al.* (2001). *Nucl. Instrum. Methods Phys. Res. A*, **467–468**, 745–747.
Giorgetti, M., Passerini, S., Smyrl, W. H. & Berrettoni, M. (1999). *Chem. Mater.* **11**, 2257–2264.
Jacquamet, L., Aberdam, D., Adrait, A., Hazemann, J. L., Latour, J. M. & Michaud-Soret, I. (1998). *Biochemistry*, **37**, 2564–2571.
Kay, M. I., Young, R. A. & Posner, A. S. (1964). *Nature (London)*, **204**, 1050–1054.
Lairda, D. F., Mucaloa, M. R. & Yokogawa, Y. (2006). *J. Colloid Interface Sci.* **295**, 348–363.

Liou, S. C., Chen, S. Y., Lee, H. Y. & Bow, J. S. (2004). *Biomaterials*, **25**, 189–196.

Okasinski, J., Cohen, J. B., Hwang, J., Mason, T. O., Ding, Z., Warschkow, O. & Ellis, D. E. (1999). *J. Am. Ceram. Soc.* **82**, 2451–2459.

Rose, J., Moulin, I., Masion, A., Bertsch, P. M., Wiesner, M. R., Bottero, J. Y., Mosnier, F. & Haehnel, F. (2001). *Langmuir*, **17**, 3658–3665.

Siritapetawee, J. & Pattanasiriwisawa, W. (2008). *J. Synchrotron Rad.* **15**, 158–161.

Sowrey, F. E., Skipper, L. J., Pickup, D. M., Drake, K. O., Lin, Z., Smith, M. E. & Newport, R. J. (2004). *Phys. Chem. Chem. Phys.* **6**, 188–192.

Touryan, L. A., Lochhead, M. J., Marquardt, B. J. & Vogel, V. (2004). *Nat. Mater.* **3**, 239–241.

Waychunas, G. A., Fuller, C. C., Davis, J. A. & Rehr, J. J. (2003). *Geochim. Cosmochim. Acta*, **67**, 1031–1043.

Wilkinson, G. (1987). *Comprehensive Coordination Chemistry*. Oxford: Pergamon.